International Journal of Nanomedicine

Dovepress
open access to scientific and medical research

Open Access Full Text Article

ORIGINAL RESEARCH

Neutral Nonenzymatic Glucose Biosensors Based on Electrochemically Deposited Pt/Au Nanoalloy Electrodes

Fang-Yu Lin[1]
Pei-Yuan Lee[1,2]
Tien-Fu Chu[3]
Chang-I Peng[3]
Gou-Jen Wang[1,3,4]

[1]Graduate Institute of Biomedical Engineering, National Chung-Hsing University, Taichung, 40227, Taiwan; [2]Department of Orthopedics, Show Chwan Memorial Hospital, Changhua, 50008, Taiwan; [3]Department of Mechanical Engineering, National Chung-Hsing University, Taichung, 40227, Taiwan; [4]Regenerative Medicine and Cell Therapy Research Center, Kaohsiung Medical University, Kaohsiung, 80708, Taiwan

Background: Type I diabetes occurs when the pancreas can only make limited or minimal insulin. Patients with type 1 diabetes need effective approaches to manage diabetes and maintain their blood-glucose concentration. Recently, continuous glucose monitoring (CGM) has been used to help control blood-glucose levels in patients with type 1 diabetes. Patients with type 2 diabetes may also benefit from CGM on multiple insulin injections, basal insulin, or sulfonylureas. Enzyme-free glucose detection in a neutral environment is the recent development trend of CGM.

Materials and Methods: Pt/Au alloy electrodes for enzyme-free glucose detection in a neutral environment were formed by electrochemically depositing Pt/Au alloy on a thin polycarbonate (PC) membrane surface with a uniformly distributed micro-hemisphere array. The PC membranes were fabricated using semiconductor microelectromechanical manufacturing processes, precision micro-molding, and hot embossing. Amperometry was used to measure the glucose concentration in PBS (pH 7.4) and artificial human serum.

Results: The Pt/Au nanoalloy electrode had excellent specificity for glucose detection, according to the experimental results. The device had a sensitivity of 2.82 μA mM^{-1} cm^{-2}, a linear range of 1.39–13.9 mM, and a detection limit of 0.482 mM. Even though the complex interfering species in human blood can degrade the sensing signal, further experiments conducted in artificial serum confirmed the feasibility of the proposed Pt/Au nanoalloy electrode in clinical applications.

Conclusion: The proposed Pt/Au nanoalloy electrode can catalyze glucose reactions in neutral solutions with enhancing sensing performance by the synergistic effect of bimetallic materials and increasing detection surface area. This novel glucose biosensor has advantages, such as technology foresight, good detection performance, and high mass production feasibility. Thus, the proposed neutral nonenzymatic glucose sensor can be further used in CGMs.

Keywords: neutral nonenzymatic glucose biosensor, Pt/Au nanoalloy electrode, electrochemical deposition, synergistic effect

Introduction

Diabetes has been a major human health problem in the twenty-first century. Type I diabetes develops when the pancreas can only produce a small amount of insulin. However, the most common type of diabetes is type 2 diabetes, which arises when the body is unable to use the insulin produced by the pancreas. Type 1 diabetes accounts for only about 5%–10% of all diabetes cases. Diabetic retinopathy, diabetic retinopathy, and diabetic nephropathy are all complications of type 1 diabetes, which also increases the risk of heart disease and stroke.[1]

Correspondence: Gou-Jen Wang
Email gjwang@dragon.nchu.edu.tw

Received: 23 May 2021
Accepted: 2 August 2021
Published: 16 August 2021

Graphical Abstract

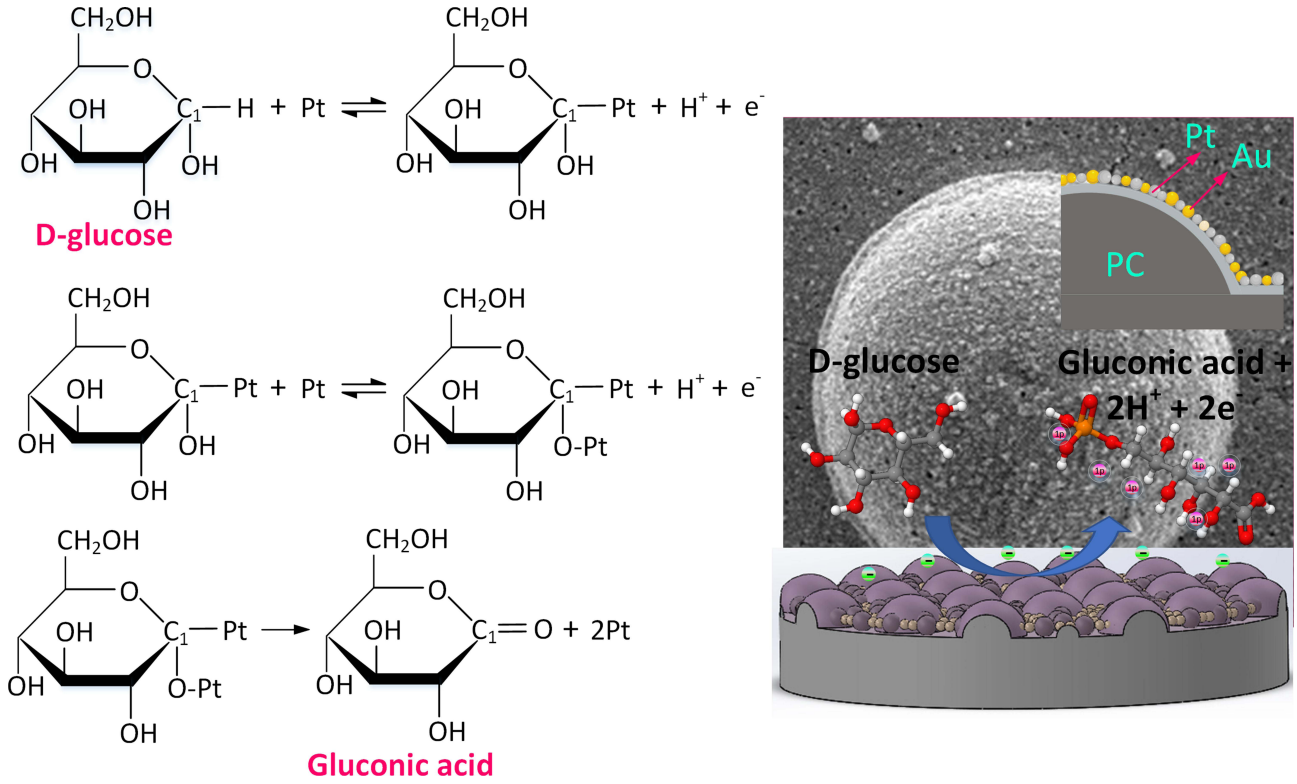

Continuous glucose monitors (CGMs) are devices for tracking glucose levels at regular intervals (varying from 5 to 15 min) 24 h a day, in which a tiny sensor wire is inserted beneath the skin of a patient.[2,3] Glucose oxidase (GOx) is generally coated on the sensor wire surface to oxidize glucose and obtain an oxidation current. The measured current signal that is proportional to the glucose concentration is subsequently transmitted to a data reader or cloud, which displays the data to the patient and/or medical doctors. CGMs have recently been used to help patients with type 1 diabetes control their blood glucose levels.[4] The measured dynamic data can be used to project glycemic trends and variability rates.[5] Using the measured data, physicians can further analyze the effects of meals, exercise, and illness on an individual's glucose levels. Patients with type 2 diabetes who are on multiple insulin injections, basal insulin, or sulfonylureas may also benefit from CGMs in addition to those with type 1 diabetes.[6,7]

The tiny sensor wire for glucose concentration detection is the most important component of a CGM. Currently approved CGMs oxidize interstitial fluid glucose molecules with enzymes to generate electric current by adopting the enzymatic technology of first-generation glucose sensors. The primarily used enzyme used is GOx.[8,9] GOx can rapidly transfer electrons through nanomaterials, but its applicability is limited by its poor long-term stability, reproducibility, environmental sensitivity, complex immobilization, and high cost.[10] Therefore, most CGMs require calibration twice a day with a confirmatory fingerstick glucose measurement. Furthermore, the GOx cofactors used in CGMs compete for oxygen with tissue oxygen, resulting in a possible overestimation of the glucose concentration in hypoxia cases.[11] Recently, nonenzymatic glucose biosensing schemes have been reported to solve the activity degradation problem of GOx and reduce vulnerability to hypoxia in current enzyme-based CGMs by utilizing the high catalytic capacity of noble metals or carbon nanotubes to provide an effective catalytic reaction area for directly oxidizing glucose to gluconolactone.

Xu et al synthesized three-dimensional (3D) Ni-doped cobalt oxide (Co_3O_4/Ni) heterostructures on a porous Ni substrate as an electrode for nonenzymatic glucose detection in an alkaline solution (0.1–3.0 M NaOH) using a hydrothermal method. A sensitivity of 13,855 μA mM^{-1} cm^{-2}, a linear range of 0.04–3.6 mM and a detection limit of 1 μM were obtained.[12] Lin et al

proposed a nonenzymatic glucose biosensor electrode with self-assembled monolayers of gold nanoparticles on a micro-hemisphere array.[13] The proposed glucose biosensor had a linear range of 1.39–13.89 mM with a sensitivity of 336.1 μA mM^{-1} cm^{-2} and a detection limit of 5.2 μM, as demonstrated by chronoamperometric (CA) glucose detection tests under alkaline conditions. The synthesized electrode had a sensitivity of 5792.7 μA mM^{-1} cm^{-2}, a low detection limit of 15 nM, and multilinear detection ranges of 15 nM–0.1 μM and 575–4098.9 μM. Sub-stoichiometric $Cu_xCo_yO_4$ nanowire framework thin-films were fabricated by Xu et al for nonenzymatic glucose detection in alkaline solutions.[14] The proposed $Cu_xCo_yO_4$ electrode had a sensitivity of 13291.7 μA mM^{-1} cm^{-2} and a detection limit of 1.36 μM, with good selectivity in serum. Ahmad et al proposed a nonenzymatic glucose biosensor based on hierarchical CuO nanoleaves. The proposed CuO nanoleaf electrode exhibited a sensitivity of 1467 μA mM^{-1} cm^{-2}, a linear range of up to 5.89 mM, and a detection limit of 12 nM in an alkaline environment.[15] More advanced alkaline nonenzymatic glucose biosensors have been recently proposed in succession.[16–20] Although the detection sensitivity and detection limit of these newly reported nonenzymatic glucose sensing schemes are greatly improved, their applications in CGMs are still limited because of their operation in alkaline solutions. Some schemes that can operate in natural solutions have also been developed.

Tarlani et al used solvothermal route-assisted amino acids to synthesize zinc oxide nanostructured electrodes for nonenzymatic glucose detection in phosphate-buffered saline (PBS) solution (pH 7.0).[21] The device had a sensitivity of 64.29 μA mM^{-1} cm^{-2}, a linear range of 1–10 mM, and a detection limit of 0.82 mM, according to experimental results. Weremfo et al proposed a nanoporous platinum electrode-based nonenzymatic electrochemical blood glucose sensor. In PBS, the nanoporous platinum electrode had a sensitivity of 5.67 μA mM^{-1} cm^{-2}, a linear range of 1–10 mM, and a detection limit of 0.8 mM.[22] Olejnik et al proposed a flexible, biocompatible electrode material based on Au nanoparticles immobilized onto titanium dimples for nonenzymatic glucose detection in neutral solutions.[23] The proposed scheme had a sensitivity of 93 μA mM^{-1} cm^{-2}, a linear range of 0.01–0.5 mM, and a detection limit of 30 μM. Wang et al used an inverse microemulsion method to synthesize monodispersed stone-like PtNi alloy nanoparticles at room temperature for nonenzymatic glucose detection.[24] The electrode had a linear range of 0.5–40 mM, a detection limit of 0.35 μM, and a sensitivity of 40.17 μA mM^{-1} cm^{-2}. Grochowska et al presented an electrode composed of gold layers deposited onto TiO_2 nanotubes formed onto flexible Ti foils, which had a sensitivity of 45 μA mM^{-1} cm^{-2}, a linear range of 0.05–3 mM, and a detection limit of 50 μM for nonenzymatic glucose detection in neutral solutions.[25] Compared to alkaline nonenzymatic glucose sensors, there are few nonenzymatic glucose sensors that can operate in neutral solutions, particularly those that can be mass-produced.

In neutral solutions, platinum has a good electrocatalytic activity for glucose. However, the intermediate products of glucose oxidation easily cover platinum electrodes, resulting in passivation, which further decreases the sensitivity of the sensor.[26] Additionally, Pt/Au metal alloys or composite materials can help to minimize the aforementioned phenomenon and improve sensing performance. Shim et al proposed a neutral nonenzymatic glucose sensor based on an Au/Pt core-shell nanoparticle electrode,[27] which had two wide dynamic ranges for glucose (0.5–10.0 μM and 0.01–10.0 mM) and a detection limit of 0.45 μM. Lin et al proposed using a bimetallic Pt/Au alloy nanomaterial electrode to fabricate an alkaline nonenzymatic glucose sensor.[28] This sensor had a wide linear detection range of 0.01–10 mM and a detection limit of 3 μM.

A neutral nonenzymatic glucose sensor based on a nanostructured Pt/Au alloy electrode is proposed in this paper. The nanostructured Pt/Au alloy electrode was formed by electrochemically depositing Pt/Au alloy on a thin polycarbonate (PC) membrane surface with a uniformly distributed micro-hemisphere array. Pt/Au alloys can catalyze glucose reactions in neutral solutions. Sensing performance can be improved by the synergistic effect of bimetallic materials, and the detection surface area of the electrode can be greatly increased by nano-/micro-hybrid Pt/Au alloy structures. Furthermore, the Pt/Au alloy is not toxic to cells. This novel glucose biosensor has advantages, such as technology foresight, good detection performance, and high mass production feasibility. Thus, the proposed neutral nonenzymatic glucose sensor can be further used in CGMs.

Materials and Methods

Sensor Fabrication

The fabrication of the proposed neutral nonenzymatic glucose biosensor based on a Pt/Au nanoalloy sensing

electrode is illustrated in Scheme 1. The first step involved the preparation of a PC membrane with a micro-hemisphere array (Scheme 1(A)). The procedure for preparing the PC is similar to that of our previous work.[29] The PC membrane was sputtered with a thin Pt layer (Scheme 1(B)) before being packaged into a sensing chip (Scheme 1(C)). Subsequently, a thin layer of Pt/Au nanoalloy was deposited onto the PC membrane via electrochemical deposition (Scheme 1(D)). Finally, a Nafion thin film was deposited onto the sensing area.

Sensor Packaging

The PC membrane that was sputtered with a Pt thin film was packaged to ensure that the sensing area of each sensing chip is identical. First, a conductive silver wire was attached to a glass slide and used as a conducting wire to connect to the PC membrane. Subsequently, to secure the sensing area, a 2×2 cm^2 parafilm with a hole (ϕ = 6 mm) was bonded to the PC membrane (Scheme 1(C)). The electrode was placed on a hot plate at 50 °C. The heated parafilm softened and tightly bonded to the electrode. Finally, to enhance the packaging efficiency, a silicon thin film was applied to the chip's surface.

Pt/Au Nanoalloy Deposition

The electrochemical deposition solution contained 1 mM $HAuCl_4$ and 2 mM H_2PtCl_6 with 0.5 M H_2SO_4 solution as the solvent.[30] To electrochemically deposit the Pt/Au nanoalloy, cyclic voltammetry (CV) was performed using an SP-150 potentiostat (Bio-Logic, USA) in a three-electrode configuration with Ag/AgCl/KCl (3 M) as the reference electrode, a Pt-wire as the counter electrode, and a working electrode with a potential scan range of −0.15 to 1.5 V and a scan rate of 100 mV/s for 20 cycles.

Nafion Thin Film Deposition

Mineral acid radicals of Nafion dissociate and become negatively charged, forming a negatively charged film on the sensor surface and generating an electrostatic effect with the anionic interference to block the interference.[31] Dropping 10 µL of 2 wt% Nafion solution on the electrode surface and allowing it to dry naturally at room temperature resulted in a Nafion thin film.

Sensor Characterization

The morphologies of the fabricated Pt/Au nanoalloy electrode were characterized by field-emission gun scanning electron microscopy (JSM-6700F, JEOL, Japan). Material characterization was conducted using a D8-discover X-ray diffractometer (Bruker, MA, USA), a dimension atomic force microscope (AFM, Bruker, MA, USA), and a PHI 5000 Versaprobe X-ray photoelectron spectrometer (XPS, ULVAC, MA, USA). The electrochemical experiments were conducted using an SP-150 potentiostat (Bio-Logic, USA). To estimate the real sensing area of the electrode, CV was conducted in a 0.1 M phosphate buffered saline

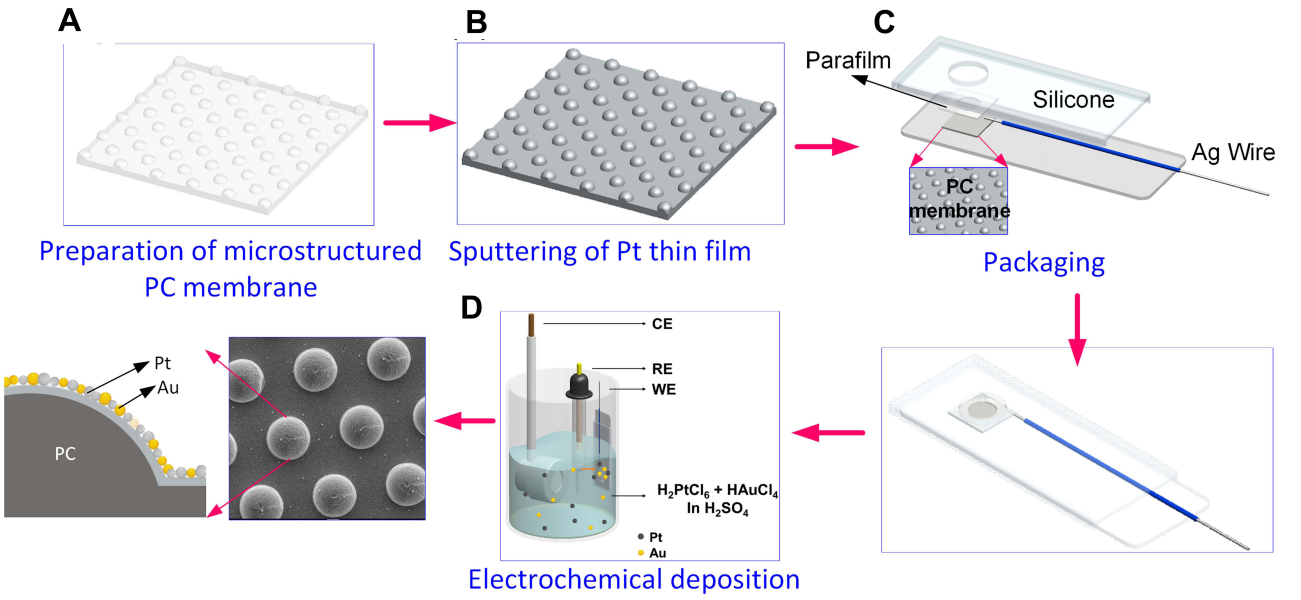

Scheme 1 Schematic of the fabrication of the proposed neutral nonenzymatic glucose biosensor: (**A**) microstructured PC membrane preparation, (**B**) Pt thin film sputtering, (**C**) packaging, and (**D**) Pt/Au nanoalloy deposition.

(PBS) solution (pH 7.0). Amperometry was used to measure the glucose concentration in PBS (pH 7.4) and artificial human serum.

Results and Discussion

Pt/Au Nanoalloy Electrode

The fabrication of the Pt/Au nanoalloy electrode is depicted in Figure 1. Figure 1A illustrates an AFM image of the concave micro-hemisphere array of the nickel mold. The concave micro-hemisphere arrays are well distributed. Figure 1B displays an SEM image of the PC membrane with a micro-hemisphere array. Using an electroformed concave nickel–cobalt mold, the micro-hemisphere array of photoresist on the original silicon surface was successfully transferred to the PC membrane via hot embossing. The cyclic voltammogram of the Pt/Au nanoalloy electrodeposition is shown in Figure 1C. Au reduction, Pt reduction, and hydrogen adsorption are the three reduction peaks. As the CV cycle increased, the reduction peak current increased, indicating that the Pt and Au nanoparticles were deposited on the PC substrate during the CV cycles. An SEM image of the Pt/Au nanoalloy-deposited PC membrane is shown in Figure 1D. The nanoparticles were uniformly distributed on the micro-hemisphere, as shown in the magnified image in the inset.

Material Characterization

As shown in Figure 2A, the XPS spectra of the as-fabricated Pt/Au nanoalloy reveal that the nanoalloy contains Pt, Au, C, and O. The energy-dispersive X-ray spectroscopy (EDS) spectrum and the element analysis table for the 2:1 nanoalloy are shown in the inset. The atomic percentages of Pt and Au were measured to be 67 and 33, respectively, indicating that the Pt/Au nanoalloy was fabricated. The X-ray diffraction (XRD) patterns of the Pt/Au nanoalloy electrodes with different Pt/Au weight ratios are

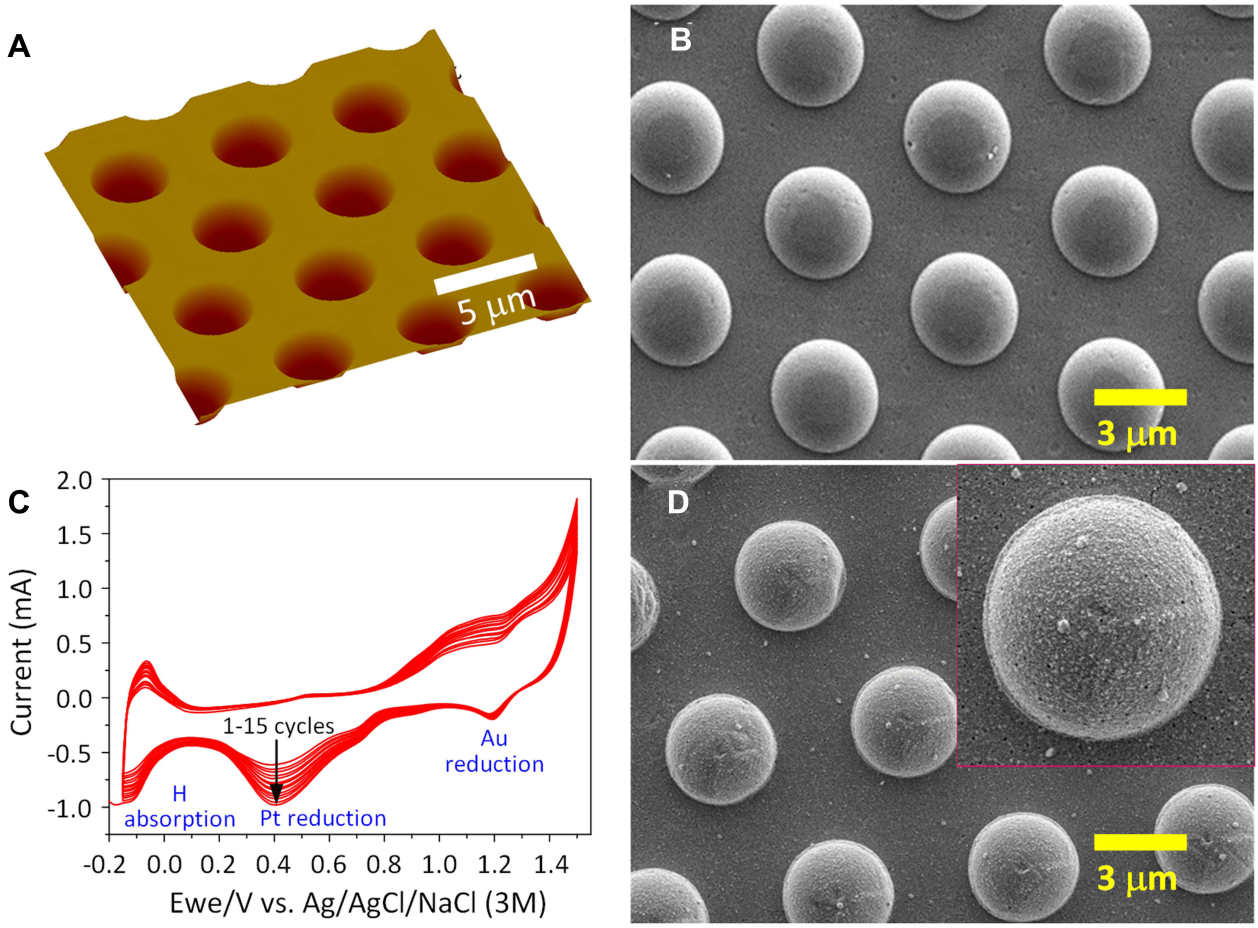

Figure 1 Fabrication results of the Pt/Au nanoalloy electrode. (**A**) AFM image of the concave micro-hemisphere array of the nickel mold, (**B**) SEM image of the PC membrane with a micro-hemisphere array, (**C**) cyclic voltammogram of Pt/Au nanoalloy electrodeposition, and (**D**) SEM image of the Pt/Au nanoalloy-deposited PC membrane.

shown in Figure 2B. At the reflection angles (2θ) of the Prague (111) crystal plane, the Pt/Au electrodes with a ratio of 2:1 have a relatively high intensity, indicating that they can catalyze the oxidation of glucose more effectively than the other Pt/Au electrodes. Figure 2C and D) show the XPS spectra of Pt and Au in the fabricated Pt/Au nanoalloy, respectively. As shown in Figure 2C, the $4f_{\frac{5}{2}}$ and $4f_{\frac{7}{2}}$ binding energies of Pt are 71.2 eV and 74.9 eV, respectively, with a 3.7 eV energy difference. The fixed intensity ratio was measured to be 0.78:1. The binding energies of the fitted Au 4f spin-orbit doublets, $4f_{\frac{5}{2}}$ and $4f_{\frac{7}{2}}$, were measured to be 83.5 eV and 87.7 eV, respectively, with a 4.2 eV energy difference, as illustrated in Figure 2D. The fixed intensity ratio was measured to be 0.75:1. The binding energies of Pt and Au in the as-fabricated Pt/Au nanoalloy appear to be lower than the binding energies of pure Pt and Au (5.65 and 5.1 eV, respectively). Therefore, glucose molecules are more likely to bind to the surface of the as-fabricated Pt/Au nanoalloy electrode.[32]

The as-fabricated Pt/Au nanoalloy was stored at room temperature for 90 d before being used to detect glucose in a neutral environment. Figure S2(A) shows the XPS spectra of the as-fabricated Pt/Au nanoalloy. As demonstrated in Figure S2(B), the $4f_{\frac{5}{2}}$ and $4f_{\frac{7}{2}}$ binding energies of Pt and the energy difference are similar to those of the original sample. Figure S2(C) shows that the binding energies of the fitted Au 4f spin-orbit doublets, $4f_{\frac{5}{2}}$ and $4f_{\frac{7}{2}}$, are 82.6

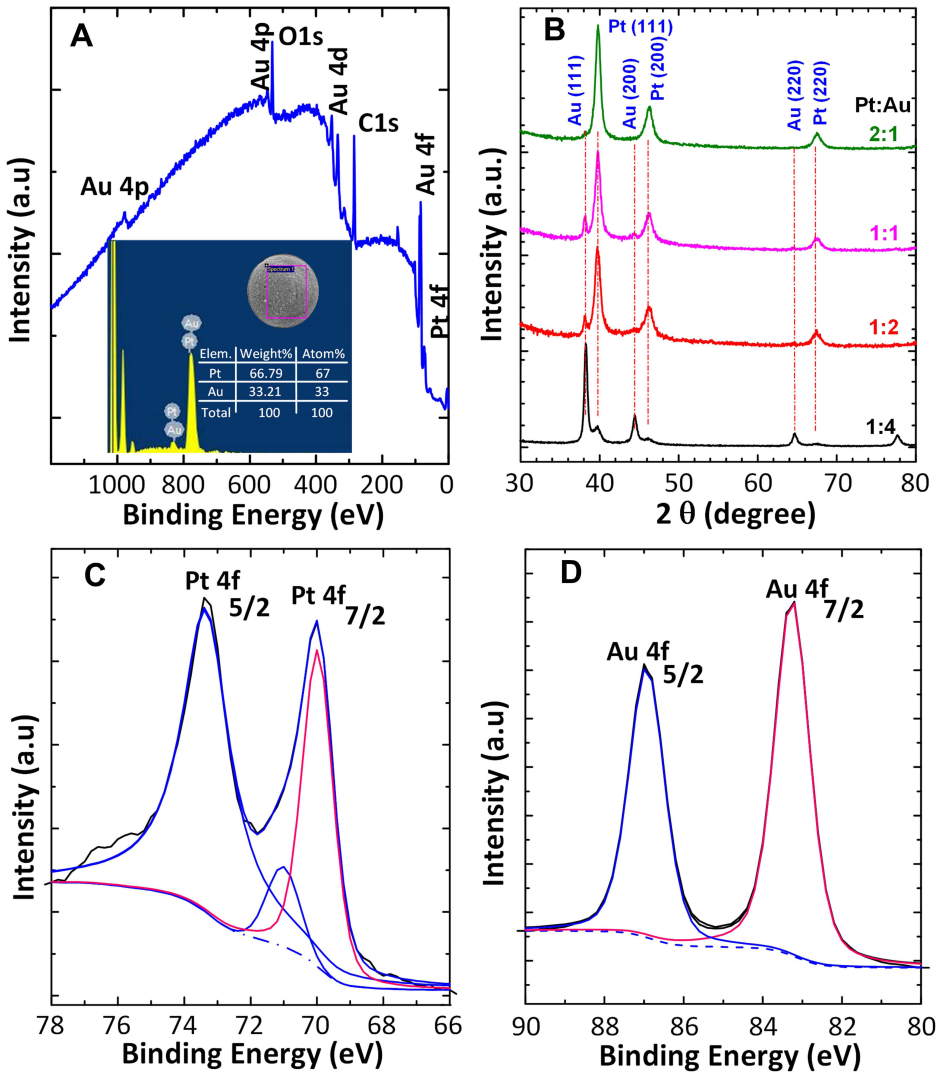

Figure 2 Material characterization. (**A**) XPS spectra of the as-fabricated Pt/Au nanoalloy. Inset: the EDS spectrum and the element analysis table for the 2:1 Pt/Au electrodes, (**B**) XRD spectra of the Pt/Au nanoalloy electrodes with different Pt/Au weight ratios, and (**C**) and (**D**) XPS spectra of Pt and Au in the as-fabricated Pt/Au nanoalloy, respectively.

eV and 86.2 eV, respectively, with a 3.7 eV energy difference, indicating that the binding energies slightly weakened.

Electrochemical Characteristics of the Electrodes

The cyclic voltammograms of the fabricated Pt/Au nanoalloy electrode and the plane Pt electrode are shown in Figure 3A. Figure 3B depicts the corresponding current versus time (*i–t*) curves. The quantity of electric charges required for complete reduction of molecules on the electrode is represented by the area below the horizontal axis (zero current) (Figure 3B). The fabricated Pt/Au nanoalloy electrode and the plane Pt have areas of 3676 and 2222 μC, respectively, below the horizontal axis. Provided that 1 cm^2 of the Pt electrode required a total charge of 210 μC to form PtO,[33] the effective electrode areas of the Pt/Au nanoalloy electrode and the plane Pt were estimated to be 17.52 cm^2 (3676 μC/210 μC) and 10.5 cm^2 (2222 μC/210 μC), respectively. The sensing area of the Pt/Au nanoalloy electrode had a 1.66-fold increase. To confirm the diffusion-controlled characteristic of a sensing electrode, the Randles–Sevcik equation (Eq. (1)) is commonly used.

$$i_p = 2.69 \times 10^5 \times n^{3/2} \times A \times C \times D^{1/2} \times v^{1/2} \quad (1)$$

The values of i_p (peak current), n (number of electrons involved in the redox couple), A (electrode area), C (analyte concentration), D (analyte diffusivity), and v (potential scan rate) are usually fixed in general applications. Hence, i_p is proportional to the square root of the scan rate. Figure 3C shows the cyclic voltammogram of the proposed Pt/Au nanoalloy electrode in a solution containing 0.1 M PBS (pH 7.4) and 11.1 mM glucose electrolyte at scan rates of 25–350 mV/s. The linear relationship between the peak current and the square root of the scan

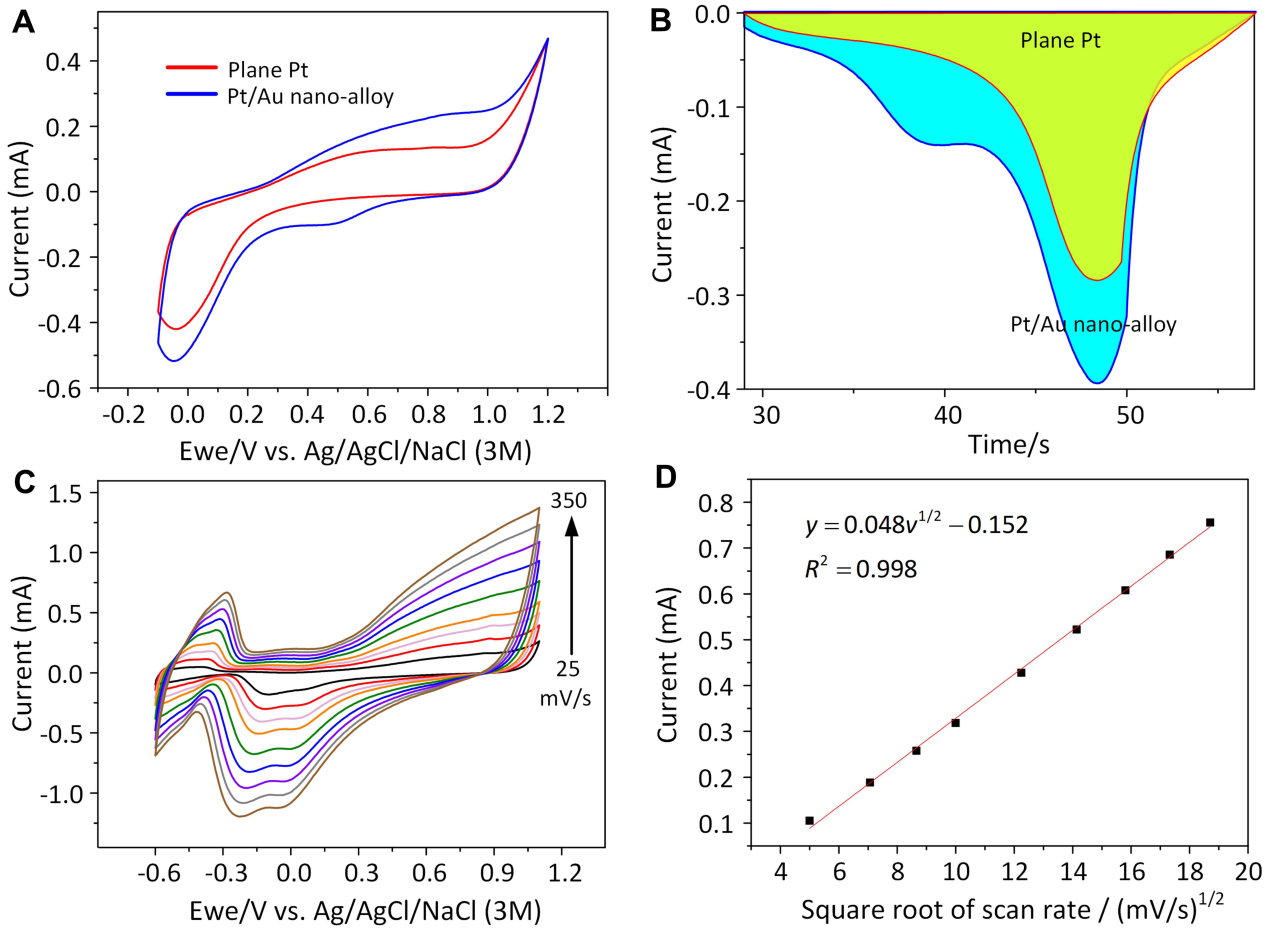

Figure 3 Electrochemical characteristics of the Pt/Au nanoalloy electrode. (**A**) Cyclic voltammograms of the Pt/Au nanoalloy electrode and the plane Pt electrode, (**B**) *i–t* curves of (**A**), (**C**) cyclic voltammogram of the Pt/Au nanoalloy electrode for scan rates of 25–350 mV/s, and (**D**) linear relationship between the peak current and the square root of the scan rate of the Pt/Au nanoalloy electrode.

rate of the as-prepared Pt/Au nanoalloy electrode is shown in Figure 3D. A typical diffusion-controlled electrochemical behavior, which is suitable for glucose detection, was exhibited by the Pt/Au nanoalloy electrode.

Pt/Au Ratio Optimization

The glucose oxidation performance of the Pt/Au nanoalloy electrode has been demonstrated to be good. The catalytic performance of alloy electrodes with different precursor deposition solution ratios (H_2PtCl_6:$HAuCl_4$) in 0.1 M PBS (pH 7.4) solution in glucose oxidation was further investigated. The cyclic voltammograms (150 mV/s) of different Pt/Au nanoalloy electrodes with different precursor deposition solution ratios in glucose oxidation are shown in Figure 4A–C). The glucose oxidation current did not have a noticeable peak. However, the glucose oxidation responses indicated by the dashed rectangle (scanning voltage of 0.4–0.6 V) in each figure can be used for performance evaluations. Figure 4D shows the oxidation current at various glucose concentrations for different H_2PtCl_6/$HAuCl_4$ ratios at a scanning voltage of 0.55 V. The current/glucose concentration relationships at H_2PtCl_6/$HAuCl_4$ ratios of 3:1 and 4:1 were included for comprehensive evaluation. At low glucose concentrations, all electrode types had a linear current/glucose concentration relationship. However, at high glucose concentrations, the nanoalloy electrode with a 2:1 H_2PtCl_6/$HAuCl_4$ ratio showed a good linear current/glucose concentration relationship. This is because the Pt and Au atom distribution in the 2:1 Pt/Au electrode allows the Pt/Au bimetallic alloy to have an improved synergistic effect. The 2:1 electrode was selected for subsequent glucose detection experiments because of its high oxidation current and sensitivity.

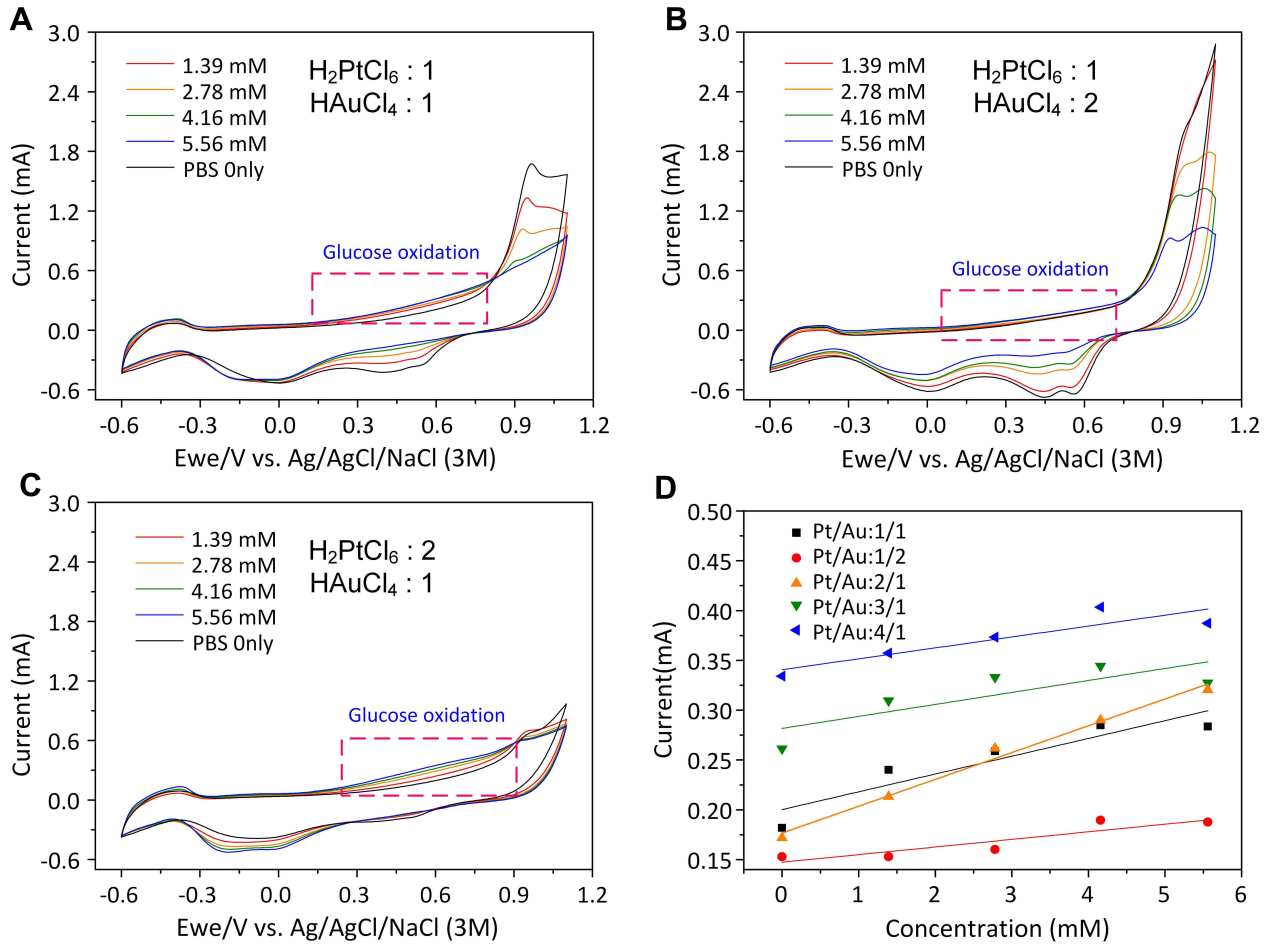

Figure 4 Catalytic performances of the alloy electrodes fabricated using different precursor deposition solution ratios: (**A**) 1:1 H_2PtCl_6/$HAuCl_4$ ratio, (**B**) 1:2 H_2PtCl_6/$HAuCl_4$ ratio, and (**C**) 2:1 H_2PtCl_6/$HAuCl_4$ ratio. (**D**) Oxidation current of various glucose concentrations for different H_2PtCl_6/$HAuCl_4$ ratios.

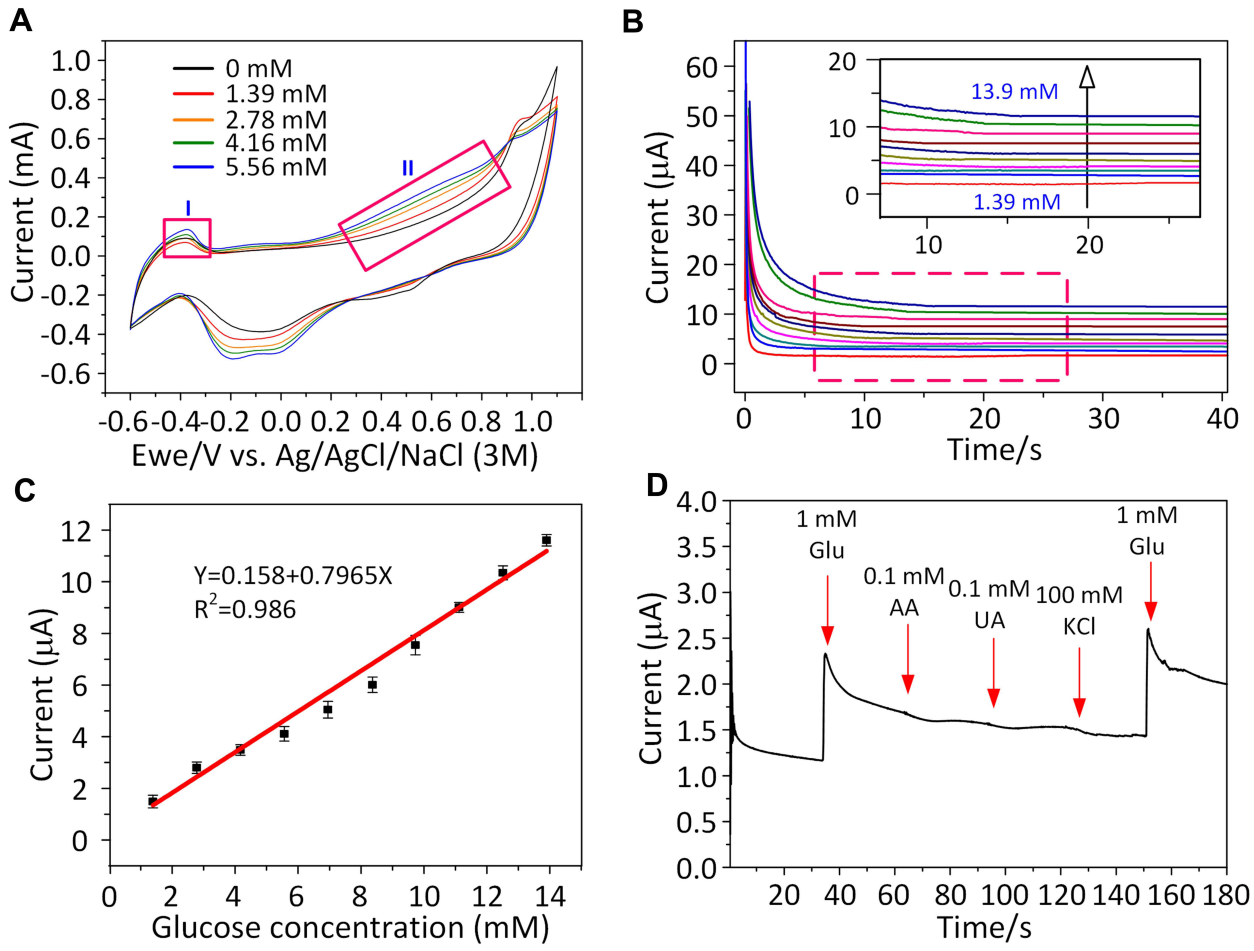

Figure 5 Nonenzymatic glucose detection in the 0.1 M PBS (pH 7.4) solution. (**A**) Cyclic voltammograms (150 mV/s) for various glucose concentrations (0–5.56 mM), (**B**) CA glucose detection results using an applied potential of 0.55 V for various glucose concentrations (1.39–13.9 mM), (**C**) linear calibration curve representing the relationship between the stable oxidation current and concentration, and (**D**) response to sequential injections of 1 mM glucose, 0.1 mM AA, 0.1 mM UA, 100 mM KCl, and 1 mM glucose.

Neutral Nonenzymatic Glucose Detection

The capability of the Pt/Au nanoalloy electrode for neutral nonenzymatic glucose detection was demonstrated by performing various experiments. Figure 5 depicts the results. Figure 5A depicts the cyclic voltammograms (150 mV/s) for various glucose concentrations (0–5.56 mM) in the 0.1 M PBS (pH 7.4) solution. The reaction between D-glucose and Pt causes the peak currents in region I. When the scanning potential was between 0.4 V and 0.6 V, the oxidation current increased as the glucose concentration increased, as shown in region II. Thus, for CA experiments, an effective glucose oxidation potential of 0.55 V was selected with the Pt/Au nanoalloy electrode.

The CA results for various glucose concentrations (1.39–13.9 mM) are shown in Figure 5B. The magnified plot from 10 s to 25 s is shown in the inset. The linear calibration curve (R^2 = 0.989) representing the relationship between the stable oxidation current at 20 s and the glucose concentration is plotted in Figure 5C. Each measurement was taken three times. The proposed electrode had a sensitivity of 2.82 μA mM^{-1} cm^{-2} and a detection limit of 0.482 mM, which was calculated according to the 3σ approach defined by the International Union of Pure and Applied Chemistry (IUPAC).[34] For clinical applications, a linear range of 1.39–13.9 mM can sufficiently cover the normal (4.4–6.6 mM) and abnormal cases of humans. Other substances in human blood, such as ascorbic acid (AA), uric acid (UA), and potassium chloride (KCl), may interfere with the measured glucose concentration signal. CA experiments were performed using a Nafion film of 2 wt% in 0.1 M PBS (pH 7.4) solution with an applied potential of 0.55 V. The responses of the Pt/Au nanoalloy electrode to sequential

injections of 1 mM glucose, 0.1 mM AA, 0.4 mM UA, 100 mM KCl, and 1 mM glucose are shown in Figure 5D. These tested interferences (AA, UA, and KCl) had minimal effect on the Pt/Au nanoalloy electrode, as indicated by the experimental results.

The long-term stability of the fabricated Pt/Au nanoalloy electrodes was further investigated using electrodes stored at room temperature for 90 d. The glucose detection results of the CA experiments for various glucose concentrations are shown in Figure S3 using the same conditions of Figure 5B. The stable currents degraded by about 20%–30%.

Operation in Artificial Human Serum

In real applications, the complex interfering species in human blood can influence the electrocatalytic oxidation of glucose. Thence, we used artificial human serum to further investigate the performance of the proposed neutral nonenzymatic glucose sensor. Figure 6 depicts the experimental results. According to the linear calibration curve presented in Figure 6B, the measured currents for each concentration decreased (Figure 6A), and the sensitivity also decreased from 2.82 to 1.34 μA mM^{-1} cm^{-2} (decreased by 52%). Although the sensing signal is expected to be degraded by the complex interfering species in human blood, the experimental results validated the feasibility of the proposed Pt/Au nanoalloy electrode in clinical applications. We propose that the construction of the linear calibration curve for clinical applications should be from the operation of the glucose sensor in human serum.

Discussion

In recent years, Pt and Au have emerged as the main electrode materials for nonenzymatic glucose detection.[35] The Au electrode has a relatively high current response, which is its principal advantage. However, as shown in Equation (2), it must be used in an alkaline environment.[36] Here, Au functions as a catalyst to increase D-glucose molecule electrochemical adsorption on the surface of Au electrodes via dehydrogenation and the direct oxidation of dehydrogenated molecules into D-gluconate ions. As shown in Equation (3), Pt electrodes can be operated in a neutral environment.[37] The Pt-based electrode is a feasible material for CGMs in a neutral environment.

$$C_6H_{12}O_6 + 2OH^- \rightarrow C_6H_{11}O_7^- + H_2O + H^+ + 2e^- \text{ and } C_6H_{12}O_6 + OH^- \rightarrow C_6H_{10}O_6 + H_2O + H^+ + 2e^- \quad (2)$$

$$\begin{aligned} &C_6H_{12}O_6 + Pt \rightarrow C_6H_{11}O_6Pt + H^+ + e^- \\ &C_6H_{11}O_6Pt + Pt \rightarrow C_6H_{10}O_6Pt_2 + H^+ + e^- \\ &C_6H_{10}O_6Pt_2 \rightarrow C_6H_{10}O_6 + 2Pt \\ &\underline{C_6H_{12}O_6 \xrightarrow{Au} C_6H_{10}O_6 + 2H^+ + 2e^-} \end{aligned} \quad (3)$$

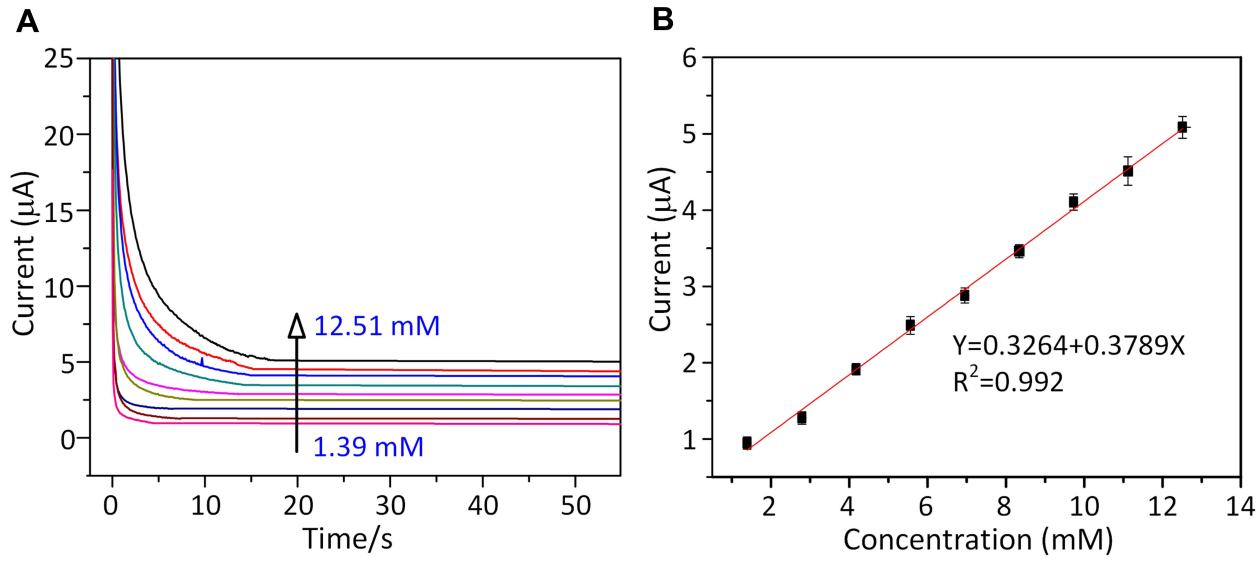

Figure 6 The performance of the proposed neutral nonenzymatic glucose sensor in artificial human serum. (**A**) Glucose detection results of CA using an applied constant voltage of 0.55 V for various glucose concentrations (1.39–12.51 mM) and (**B**) linear calibration curve representing the relationship between the stable oxidation current and concentration.

Figure 7 further illustrates the sensing mechanism described in Equation (3).

To enhance the catalytic performance of Pt and improve chlorine poisoning during the catalytic process, Au can change the electronic energy band structure of Pt by changing the strength of the molecules adsorbed on the surface.[38] Figure S1 shows a comparison of the nonenzymatic glucose detection of the micro-hemisphere array PC membrane deposited with Au, Pt, and Pt/Au nanoalloy in a neutral environment (PBS, pH 7.4). Even with a high glucose concentration (11.1 mM), the Au electrode did not exhibit any catalytic response in a neutral environment, as shown in Figure S1(A). Figure S1(B) depicts the catalytic response of the Pt electrode. The oxidation current did not significantly increase after 11.1 mM glucose was added. This result can be attributed to the Pt electrode being easily covered by glucose oxidation products, which results in a decrease in its catalytic efficiency. For the Pt/Au nanoalloy electrode, the oxidation current noticeably increased in the scanning potential range of 0.4–0.7 V after glucose was added (Figure S1(C)). To confirm the attachment stability of the electrochemically deposited Pt/Au nanoalloy, the Pt/Au nanoalloy electrode was placed in PBS containing 5 mM $Fe(CN)6^{3-/4-}$. The electrode surface was scanned continuously for 200 cycles using CV at a scan rate of 100 mV/s. The attachment stability of the Pt/Au nanoalloy is indicated by the results in Figure S1(D).

In recent years, nanostructured electrodes have been widely used to develop nonenzymatic glucose biosensors. However, because they require alkaline solutions, their actual use in CGMs is limited. Thus, several neutral nonenzymatic schemes have been developed. In Table 1, the sensitivity, detection limit, and linear range of the proposed Pt/Au nanoalloy electrode for neutral nonenzymatic glucose sensing are compared to those of other recently developed neutral nonenzymatic glucose biosensors. Overall, the functional properties of the proposed biosensor were relatively good.

Conclusions

Patients with type 1 diabetes require effective methods for managing their diabetes and maintaining their blood glucose levels. CGMs have recently been used to help patients with type 1 diabetes control their blood glucose levels. The recent development trend in CGMs is enzyme-free glucose detection in a neutral environment. To develop neutral nonenzymatic glucose biosensors based on a Pt/Au nanoalloy electrode, we used Taiwan's excellent industrial processes, such as

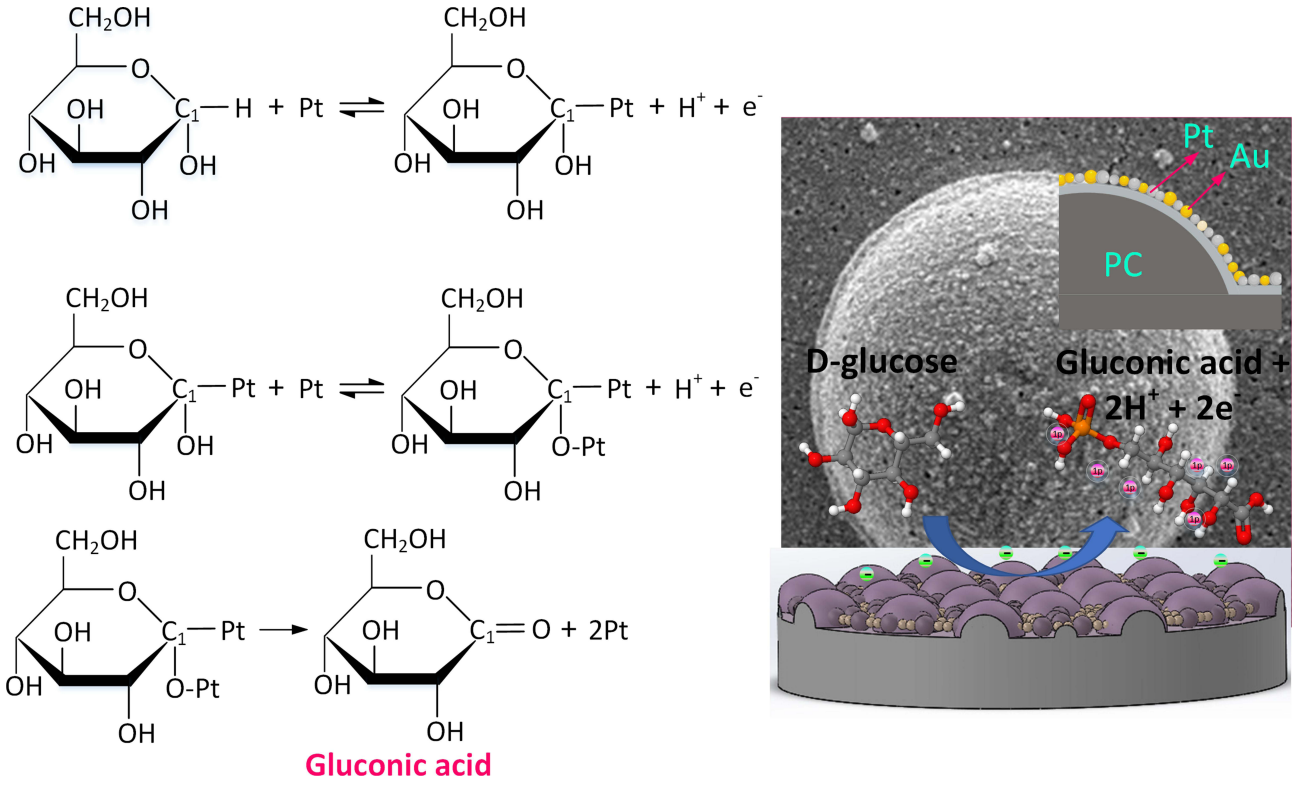

Figure 7 The sensing mechanism of the proposed Pt/Au nanoalloy electrode in glucose detection.

Table 1 Neutral Non-Enzymatic Glucose Biosensors and Their Functional Properties

Electrode	Sensitivity ($\mu A\ mM^{-1}\ cm^{-2}$)	LOD (μM)	Linear Range (mM)	Reference
ZnO nanostructures	64.29	820	1–10	[16]
Nanoporous Pt	5.67	800	1–10	[17]
Au-dimpled Ti structures	93	30	0.01–0.5	[18]
TiO2–Au composite	45	50	0.05–3	[20]
Au@Pt/Au NPs	2.94	3	0.01–10	[22]
Carbon nano-onions	26.5	210	1–10	[39]
Pt black	1.62	50	2–36	[40]
Pt/Au/Boron-Doped Diamond	Not provided	6.5	0.01–6.5	[41]
Pt/Au nano-alloy	**2.82**	**482**	**1.39–13.9**	**This work**

semiconductor microelectromechanical manufacturing processes, precision micro-molding, hot embossing, and chip packaging. The Pt/Au nanoalloy electrode had excellent specificity for glucose detection, according to the experimental results. The device had a sensitivity of 2.82 $\mu A\ mM^{-1}\ cm^{-2}$, a linear range of 1.39–13.9 mM, and a detection limit of 0.482 mM. Even though the complex interfering species in human blood can degrade the sensing signal, further experiments conducted in artificial serum confirmed the feasibility of the proposed Pt/Au nanoalloy electrode in clinical applications. Therefore, we recommend constructing the linear calibration curve for clinical applications using its operation in human serum.

Acknowledgments

The authors would like to offer their appreciation to the Ministry of Science and Technology of Taiwan under grant number MOST-109y-002 & MOST-107-2923-E-005-001-MY3 for their financial support of this research.

Disclosure

The authors report no conflicts of interest in this work.

References

1. Medical News Today. An overview of diabetes types and treatments, [Internet]; 2020. Available from: https://www.medicalnewstoday.com/articles/323627. Accessed August 3, 2021.
2. Klonoff DC, Ahn D, Drincic A. Continuous glucose monitoring: a review of the technology and clinical use. *Diabetes Res Clin Pract*. 2017;133:178–192. doi:10.1016/j.diabres.2017.08.005
3. Rodbard D. Continuous glucose monitoring: a review of recent studies demonstrating improved glycemic outcomes. *Diabetes Technol Ther*. 2017;19:S25–S37. doi:10.1089/dia.2017.0035
4. Bertachi A, Ramkissoon CM, Bondia J, Vehí J. Automated blood glucose control in type 1 diabetes: a review of progress and challenges. *Endocrinol Diabetes Nutr*. 2018;65:172–181. doi:10.1016/j.endinu.2017.10.011
5. Ekhlaspour L, Tabatabai I, Buckingham B. A review of continuous glucose monitoring data interpretation in the age of automated insulin delivery. *J Diabetes Sci Technol*. 2019;13:645–663. doi:10.1177/1932296819851790
6. Vettoretti M, Facchinetti A. Combining continuous glucose monitoring and insulin pumps to automatically tune the basal insulin infusion in diabetes therapy: a review. *Biomed Eng Online*. 2019;18:37. doi:10.1186/s12938-019-0658-x
7. Ajjan RA, Jackson N, Thomson SA. Reduction in HbA1c using professional flash glucose monitoring in insulin treated type 2 diabetes patients managed in primary and secondary care settings: a pilot, multicentre, randomised controlled trial. *Diabetes Vasc Dis Res*. 2019;16:385–395. doi:10.1177/1479164119827456
8. Chen C, Xie Q, Yang D, et al. Recent advances in electrochemical glucose biosensors: a review. *RSC Adv*. 2013;3:4473–4491. doi:10.1039/c2ra22351a
9. Kim J, Campbell AS, Wang J. Wearable non-invasive epidermal glucose sensors: a review. *Talanta*. 2018;177:163–170. doi:10.1016/j.talanta.2017.08.077
10. Park S, Boo H, Chung TD. Electrochemical non-enzymatic glucose sensors. *Anal Chim Acta*. 2006;556:46–57. doi:10.1016/j.aca.2005.05.080
11. Rebel A, Rice MA, Fahy BG. Accuracy of point-of-care glucose measurements. *J Diabetes Sci Technol*. 2012;6:396–411. doi:10.1177/193229681200600228
12. Xu H, Xia C, Wang S, et al. Electrochemical non-enzymatic glucose sensor based on hierarchical 3D Co_3O_4/Ni heterostructure electrode for pushing sensitivity boundary to a new limit. *Sens Actuators B Chem*. 2018;267:93–103. doi:10.1016/j.snb.2018.04.023
13. Lin YC, Liao S, Huang T, Wang GJ. A novel biosensor electrode with self-assembled monolayer of gold nanoparticle on a micro hemisphere array. *J Electrochem Soc*. 2019;166:B349–B354. doi:10.1149/2.0361906jes
14. Xu H, Han F, Xia C, Wang S, Zhuiykov S, Zheng G. Spinel sub-stoichiometric $Cu_xCo_yO_4$ nano-wire framework thin-film electrode for enhanced electrochemical non-enzymatic sensing of glucose. *Electrochim Acta*. 2020;331:135295. doi:10.1016/j.electacta.2019.135295
15. Ahmad R, Khan M, Mishra P, et al. Engineered hierarchical CuO nanoleaves based electrochemical nonenzymatic biosensor for glucose detection. *J Electrochem Soc*. 2021;168:017501. doi:10.1149/1945-7111/abd515
16. Gumilar G, Kaneti YV, Henzie J, et al. General synthesis of hierarchical sheet/plate-like M-BDC (M = Cu, Mn, Ni, and Zr) metal–organic frameworks for electrochemical non-enzymatic glucose sensing. *Chem Sci*. 2020;11:3644–3655. doi:10.1039/C9SC05636J

17. Yuan G, Yu S, Jie J, Wang C, Li Q, Pang H. Cu/Cu_2O nanostructures derived from copper oxalate as high performance electrocatalyst for glucose oxidation. *Chin Chem Lett*. 2020;31(7):1941–1945. doi:10.1016/j.cclet.2019.12.034
18. Bag S, Baksi A, Nandam SH, et al. Nonenzymatic glucose sensing using $Ni_{60}Nb_{40}$ nanoglass. *ACS Nano*. 2020;14(5):5543–5552. doi:10.1021/acsnano.9b09778
19. Waqas M, Wu L, Tang H, et al. Cu2O microspheres supported on sulfur-doped carbon nanotubes for glucose sensing. *ACS Appl Nano Mater*. 2020;3(5):4788–4798. doi:10.1021/acsanm.0c00847
20. Gu J, Xu Y, Li Q, Pang H. Porous Ni/NiO nanohybrids for electrochemical catalytic glucose oxidation. *Chin Chem Lett*. 2021;32(6):2017–2020. doi:10.1016/j.cclet.2020.11.066
21. Tarlani A, Fallah M, Lotfi B, et al. New ZnO nanostructures as non-enzymatic glucose biosensors. *Biosens Bioelectron*. 2015;67:601–607. doi:10.1016/j.bios.2014.09.063
22. Weremfo A, Fong STC, Khan A, Hibbert DB, Zhao C. Electrochemically roughened nanoporous platinum electrodes for non-enzymatic glucose sensors. *Electrochim Acta*. 2017;231:20–26. doi:10.1016/j.electacta.2017.02.018
23. Olejnik A, Siuzdak K, Karczewski J, Grochowska KA. flexible Nafion coated enzyme-free glucose sensor based on Au-dimpled Ti structures. *Electroanalysis*. 2020;32:323–332. doi:10.1002/elan.201900455
24. Wang R, Liang X, Liu H, Cui L, Zhang X, Liu C. Non-enzymatic electrochemical glucose sensor based on monodispersed stone-like PtNi alloy nanoparticles. *Microchim Acta*. 2018;185:339. doi:10.1007/s00604-018-2866-7
25. Grochowska K, Ryl J, Karczewski J, Śliwiński G, Cenian A, Siuzdak K. Non-enzymatic flexible glucose sensing platform based on nanostructured TiO_2–Au composite. *J Electroanal Chem*. 2019;837:230–239. doi:10.1016/j.jelechem.2019.02.040
26. Si P, Huang Y, Wang T, Ma J. Nanomaterials for electrochemical non-enzymatic glucose biosensors. *RSC Adv*. 2013;3:3487–3502. doi:10.1039/c2ra22360k
27. Shim K, Lee W, Park M, et al. Au decorated core-shell structured Au@Pt for the glucose oxidation reaction. *Sens Actuators B Chem*. 2019;278:88–96. doi:10.1016/j.snb.2018.09.048
28. Lin L, Weng S, Zheng Y, et al. Bimetallic PtAu alloy nanomaterials for nonenzymatic selective glucose sensing at low potential. *J Electroanal Chem*. 2020;865:114147. doi:10.1016/j.jelechem.2020.114147
29. Wang D, Cui X, Xiao Q, et al. Electronic behaviour of Au-Pt alloys and the 4f binding energy shift anomaly in Au bimetallics- X-ray spectroscopy studies. *AIP Adv*. 2018;8:065210. doi:10.1063/1.5027251
30. Hu Y, Zhang H, Wu P, Zhang H, Zhou B, Cai C. Bimetallic Pt-Au nanocatalysts electrochemically deposited on graphene and their electrocatalytic characteristics towards oxygen reduction and methanol oxidation. *Phys Chem Chem Phys*. 2011;13:4083–4094. doi:10.1039/c0cp01998d
31. Yuan JH, Wang K, Xia XH. Highly ordered platinum-nanotubule arrays for amperometric glucose sensing. *Adv Funct Mater*. 2005;15:803–809. doi:10.1002/adfm.200400321
32. Pasta M, La Mantia F, Cui Y. Mechanism of glucose electrochemical oxidation on gold surface. *Electrochim Acta*. 2010;55:5561–5568. doi:10.1016/j.electacta.2010.04.069
33. Singh B, Laffir F, McCormac T, Dempsey E. PtAu/C based bimetallic nanocomposites for non-enzymatic electrochemical glucose detection. *Sens Actuators B Chem*. 2010;150:80–92. doi:10.1016/j.snb.2010.07.039
34. Nantaphol S, Watanabe T, Nomura N, Siangproh W, Chailapakul O, Einaga Y. Bimetallic Pt-Au nanocatalysts electrochemically deposited on boron-doped diamond electrodes for nonenzymatic glucose detection. *Biosens Bioelectron*. 2017;98:76–82. doi:10.1016/j.bios.2017.06.034
35. He W, Sun Y, Xi J, Abdurhman AAM, Ren J, Duan H. Printing graphene-carbon nanotube-ionic liquid gel on graphene paper: towards flexible electrodes with efficient loading of PtAu alloy nanoparticles for electrochemical sensing of blood glucose. *Anal Chim Acta*. 2016;903:61–68. doi:10.1016/j.aca.2015.11.019
36. Long GL, Winefordner JD. Limit of detection-a closer look at the IUPAC definition. *Anal Chem*. 1983;55:712A–724A.
37. Mohapatra J, Ananthoju B, Nair V, et al. Enzymatic and non-enzymatic electrochemical glucose sensor based on carbon nano-onions. *Appl Surf Sci*. 2018;442:332–341. doi:10.1016/j.apsusc.2018.02.124
38. Lee S, Yoon H, Xuan X, Park JY, Paik S, Allen MG. A patch type non-enzymatic biosensor based on 3D SUS micro-needle electrode array for minimally invasive continuous glucose monitoring. *Sens Actuators B Chem*. 2016;222:1144–1151. doi:10.1016/j.snb.2015.08.013
39. Chu TF, Rajendran R, Kuznetsova I, Wang GJ. High-power, non-enzymatic glucose biofuel cell based on a nano/micro hybrid-structured Au anode. *J Power Sources*. 2020;453:227844. doi:10.1016/j.jpowsour.2020.227844
40. Thiagarajan S, Chen SM. Preparation and characterization of PtAu hybrid film mdified electrodes and their use in simultaneous determination of dopamine, ascorbic acid and uric acid. *Talanta*. 2007;74:212–222. doi:10.1016/j.talanta.2007.05.049
41. Cadle SH, Bruckenstein S. Ring-disk electrode study of the reduction of bismuth on platinum. *Anal Chem*. 1972;44:1993–2001. doi:10.1021/ac60320a011